Line-Edge Roughness performance targets for EUV Lithography

Timothy A. Brunner[*a], Xuemei Chen[b], Allen Gabor[a], Craig Higgins[b], Lei Sun[c], Chris A. Mack[d]
[a]GLOBALFOUNDRIES, Hopewell Junction, NY 12533
[b]GLOBALFOUNDRIES, Malta, NY
[c]GLOBALFOUNDRIES, Albany, NY
[d]Fractilia, 1605 Watchhill Rd, Austin, TX 78703

ABSTRACT

Our paper will use stochastic simulations to explore how EUV pattern roughness can cause device failure through rare events, so-called "black swans". We examine the impact of stochastic noise on the yield of simple wiring patterns with 36nm pitch, corresponding to 7nm node logic, using a local Critical Dimension(CD)-based fail criteria Contact hole failures are examined in a similar way. For our nominal EUV process, local CD uniformity variation and local Pattern Placement Error variation was observed, but no pattern failures were seen in the modest (few thousand) number of features simulated. We degraded the image quality by incorporating Moving Standard Deviation (MSD) blurring to degrade the Image Log-Slope(ILS), and were able to find conditions where pattern failures were observed. We determined the Line Width Roughness (LWR) value as a function of the ILS. By use of an artificial "step function" image degraded by various MSD blur, we were able to extend the LWR vs ILS curve into regimes that might be available for future EUV imagery. As we decreased the image quality, we observed LWR grow and also began to see pattern failures. For high image quality, we saw CD distributions that were symmetrical and close to Gaussian in shape. Lower image quality caused CD distributions that were asymmetric, with "fat tails" on the low CD side (under-exposed) which were associated with pattern failures. Similar non-Gaussian CD distributions were associated with image conditions that caused missing contact holes, i.e. CD=0.

Keywords: EUV Lithography, Line Edge Roughness, Line Width Roughness, Pattern Defects, Yield, Local CD Uniformity, Stochastic Resist Models

1. INTRODUCTION

As EUV lithography[1] comes closer to High Volume Manufacturing, there is a strong drive to understand and improve every aspect of patterning precision. One important area of concern for EUV is Line Edge Roughness(LER) issues caused by stochastic noise. Such stochastic noise is present for all lithographic processes but is more worrisome for EUV lithography for several reasons:

- fewer photons per unit dose, since each EUV photon carries 14X more energy than a 193nm photon
- limited EUV power – only a fraction (≈1%) of the source power at intermediate focus makes it to the wafer
- only a fraction of EUV photons are actually absorbed within the resist, typically <20% for polymer materials
- smaller features as we progress to more advanced nodes, and so less area to collect EUV photons. Ideally, as the lithographic pixel size shrinks, the number of photons per pixel would stay the same.

The most fundamental solution to stochastic noise is to increase the exposure dose, with difficult throughput and economic implications. The "triangle of death" tradeoff between LER, dose and resolution[2] is being thoroughly explored by the industry[3], and has a strong theoretical foundation[4]. Future EUV needs may require kilowatt sources[5], and perhaps drive the development of Free Electron Laser sources[6]. A key metric of process capability is the Edge Placement Error[5, 7] (EPE) which appropriately combines CD variability, overlay variability and LER to summarize the accuracy of placing each

[*] Email: Timothy.brunner@globalfoundries.com

Extreme Ultraviolet (EUV) Lithography VIII, edited by Eric M. Panning, Kenneth A. Goldberg, Proc. of SPIE
Vol. 10143, 101430E · © 2017 SPIE · CCC code: 0277-786X/17/$18 · doi: 10.1117/12.2258660

Downloaded From: http://proceedings.spiedigitallibrary.org/ on 06/07/2017 Terms of Use: http://spiedigitallibrary.org/ss/termsofuse.aspx

pattern edge. Stochastic noise impacts all three components of EPE, causing local CD non-uniformity, local pattern placement errors as well as LER.

A standard LER description[8] uses three parameters: a 3σ magnitude of the LER, a correlation length L_C and a roughness exponent α. SEM images are the most common LER metrology, but it is not so easy to extract accurate LER data[9]. The ebeam can interact with the photoresist to change the resist shape, i.e. "resist shrinkage". (This is less of a problem with measuring edges etched into some inorganic material.) The SEM scan direction causes significant image asymmetry, such that the left edge and the right edge look quite different[10]. In this paper, such real world metrology issues are avoided by using lithography simulation to explore stochastic noise in an EUV process. In recent years, tremendous progress has been made on accurate stochastic resist models[11-13]. Such models have been used to better understand EUV pattern printability limits[14] and EUV contact hole CD distributions[15]. This paper will make a fundamental assumption that the stochastic resist model we use is accurately representing an actual EUV exposure process. The experimental data supporting this assumption will not be presented here.

2. STOCHASTIC EUV RESIST SIMULATIONS OF LONG LINES

In our simulations, we mimic an NXE 3300 EUV expose tool with λ=13.5nm and NA=0.33. We use a standard illumination mode called Q25, which is a Quasar shape with 25° blade angle. The 3D mask calculation uses an 80nm thick Ta-based absorber, and a carefully calibrated multi-layer which includes diffused areas between the Moly and Si bilayers. We assumed a positive-tone, chemically-amplified resist coated to a 30nm thickness on top of an organic under-layer. A grating pattern with 36nm pitch and reflector width of 17.5nm was assumed (these are 1X wafer dimensions) targeting approximately 18nm trenches in the resist. A key component for this study is the stochastic resist model[11-13] of the PROLITH™ simulation software, whose parameters were adjusted to match experimental results for a particular resist process of interest to us. The dose-to-size is approximately $44mJ/cm^2$ for the nominal process conditions assumed here. Fig. 1 illustrates the major steps in the simulation. First, an aerial image profile is calculated, which like most OPC or simulation software is a continuum model, using the average value of the intensity at each point. Next, a stochastic latent image is created, driven by discrete EUV photon absorption events. Next, the Post-Expose Bake (PEB) process drives reaction-diffusion which creates a deblocked polymer profile, and the deblocked polymer is developed away to create the final developed profile.

.

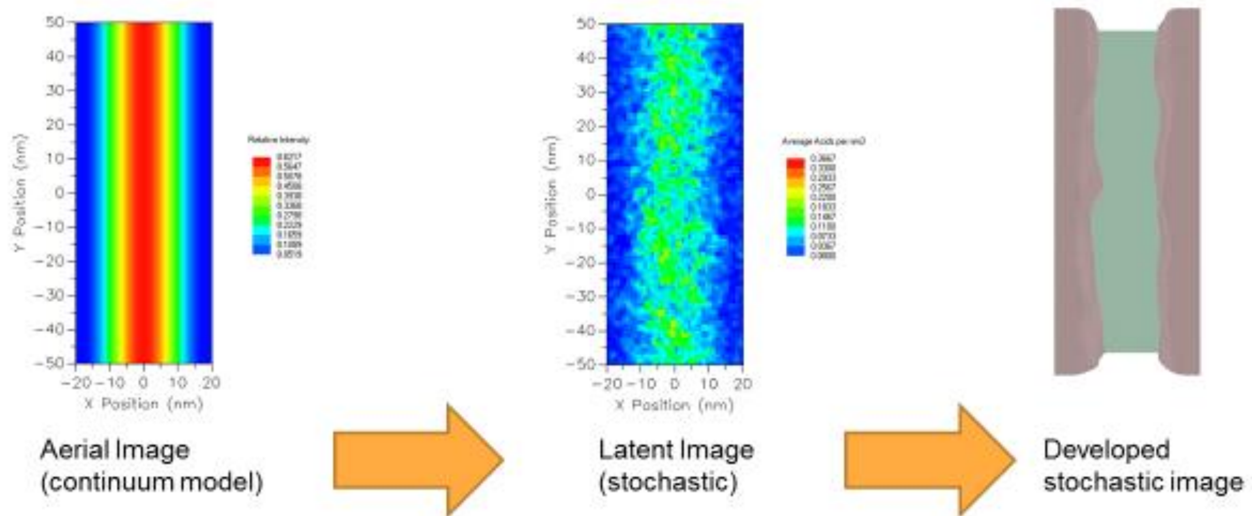

Figure 1. Stochastic image simulation flow for the case of EUV imaging of a long trench with 36nm pitch. The aerial image is first calculated as a smooth profile. Next a stochastic calculation of the latent image before PEB showing the photoacid concentration. Finally, the PEB drives deblocking reactions which create the final profile after development.

Downloaded From: http://proceedings.spiedigitallibrary.org/ on 06/07/2017 Terms of Use: http://spiedigitallibrary.org/ss/termsofuse.aspx

Now that we have determined a 3D developed resist profile, we measure many slices along the length of the line. In order to get high resolution determination of roughness, we slice every 1nm along the line. At each slice position (y), we determine the left edge position $X_L(y)$ and the right edge position $X_R(y)$ at the point where the resist thickness is 3nm, or 10% of the full resist height. Having determined the edges, the local Critical Dimension $CD(y) = X_R(y) - X_L(y)$ as well as the local Pattern Placement Error $PPE(y) = (X_R(y) + X_L(y))/2$ are calculated. Many data points are needed to get valid roughness characterization. We always assume an infinitely long line, so there are never line ends to worry about. But we can only sample a finite number of points for each individual stochastic simulation. We typically run 100 lines of length 500nm for each process condition, but get very similar results with 25 lines of length 2000nm. There are several measures of roughness we are interested in, including:

- LER_L and LER_R which are the 3σ measures of the deviation of the left and right edges
- LWR which is a 3σ measure of the variation of the local CD along the long line
- Pattern Placement Roughness (PPR) which is a 3σ measure of the variation of the local PPE, i.e. the center line.

Along with these measures of lateral roughness, we also calculate two other standard roughness parameters: Correlation Length L_C and roughness exponent α, using the Height-Height Correlation Function method[16].

In order to estimate the yield impact of roughness, we need criteria for pattern acceptability. Let's imagine that this trench line is used as an interconnect wire. An "open" error would occur if the wire locally pinches shut. For this paper, we will assume any local CD less than 5nm would represent an "open" fail. Similarly, a "short" fail can occur if the local CD is too large, causing the inter-wire dielectric to be too narrow, and so we designate local CD >30nm to be unacceptable. The pattern yield is then summarized[14] with the fraction of unacceptable "Not OK" slices (%NOK) based on the number of failing slices relative to the total number of slices.

Table 1 lists key parameters determined for our 36nm pitch pattern at best focus and best dose. We find that the left and right edges typically have low correlation, and so we can regard X_L and X_R as independent random variables. Under this assumption,

$$LWR = 3\times\sqrt{Var(X_R - X_L)} = \sqrt{2}\,LER,$$

and

$$PPR = 3\times\sqrt{Var((X_R + X_L)/2)} = \sqrt{2}\,LER/2.$$

The calculated ratios of LWR, PPR and LER are close to these expectations. (This assumption of low correlation may break down under some circumstances.) The correlation length L_C is about 8nm, somewhat smaller than typical immersion resist values, and the exponent α of 0.82 lies in the typical range between 0.5 and 1.

Mean CD	18.73nm
LER_L	2.58nm
LER_R	2.58nm
LWR	3.76nm
PPR	1.77nm
LWR L_C	8.02nm
LWR α	0.82
%NOK	0%

Table 1. Key metrics calculated for the nominal process, based on 100 trenches, each 500nm long

The %NOK value is 0, since this nominal EUV printing situation is very robust against the yield criteria we have set. The total line length we have examined, 50 microns, is many orders of magnitude smaller than that needed for an advanced chip. So how can we examine questions of LER impact on yield with practical simulation runs? We take the approach of degrading the process such that failures occur at a detectable rate, a philosophy similar to chip reliability tests using high temperature to accelerate device failures. Our process degradation mechanism of choice is the use of stage vibration, i.e. Moving Standard Deviation (MSD), where we assume a Gaussian blur distribution. Such a blur can be representative of a wide range of actual image blur mechanisms, including defocus, acid diffusion, image fading, stage vibrations, etc.

Downloaded From: http://proceedings.spiedigitallibrary.org/ on 06/07/2017 Terms of Use: http://spiedigitallibrary.org/ss/termsofuse.aspx

Fig. 2 plots the Image Log-Slope (ILS) as a function of the MSD blur as triangles. At the lowest MSD value of 1nm, the ILS is roughly 147/micron, and the ILS decreases with increasing MSD blur. For full generality, we would like to also explore larger values of ILS than our assumed EUV imagery, since higher NA, improved masks, more highly optimized source shapes or other EUV imaging improvements are likely in the future. Rather than trying to guess about future advanced EUV imagery details, we simply assume a super-sharp step function image that goes from zero to full intensity in one grid point of 1nm. While such an image can never be practically achieved, we can again utilize MSD blur to bring down the ILS to any desired value of interest. The data points from the MSD blurred step function image are shown as red circles in Fig 2. In this manner, any desired ILS value can be achieved for the 36nm pitch image.

Full stochastic simulation sets were run using these images with many different ILS. Fig. 3 shows how LWR varies at the different blur values. The data points are plotted against the quantity 0.2/ILS, showing a smooth curve with a substantial range of simple linear dependence. 0.2/ILS has a simple interpretation as the CD change from a 10% dose change, under the assumption of a simple resist threshold model. It is note-worthy that both the normal EUV imagery data and the step function imagery data fall on the same universal curve of LWR versus 0.2/ILS for this particular stochastic resist model. At the extreme left of Fig. 3 there is a very interesting data point at the highest ILS value of 1020/micron, nearly 7X larger than the nominal EUV projection image value. The LWR for this extreme image is 2.26nm, as compared to the 3.76nm value for normal EUV imagery. Unfortunately, experimental verification of the LWR for this super-sharp image is very difficult, if not impossible.

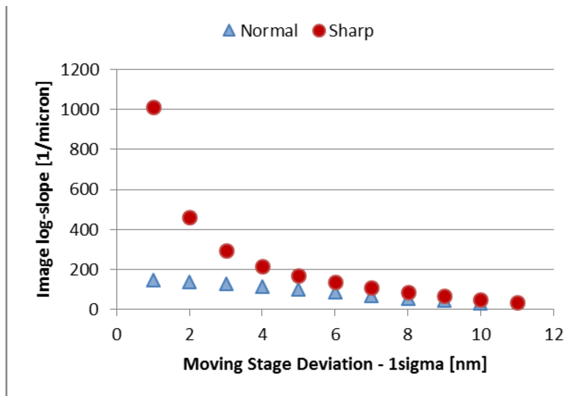

Figure 2 Image Log-slope for various MSD blurs. The triangles represent the normal EUV imaging, while the circles represent an artificial step function image.

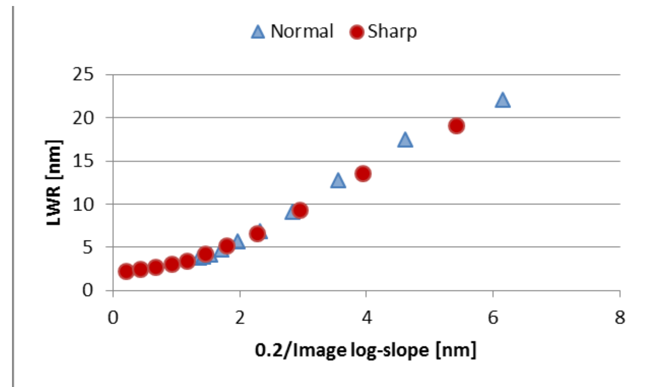

Figure 3. LWR versus 0.2/ILS for different values of MSD blur. The data points for the degraded normal image and the degraded artificial step function image fall on the same curve.

Now we examine the %NOK for the MSD-degraded imagery, plotted in Fig. 4 against the LWR value. Once again we find both normal and step function images lie on the same curve, so ILS and LWR correlate strongly with %NOK. For ease of seeing small values, we have plotted on a log-scale, and therefore all the %NOK=0 points for LWR<4.8nm are omitted. While %NOK values of .01% would seem to be very good, keep in mind that this value means that several out of spec local CDs occurred on a line length totaling a mere 50 microns, far less than would be required in real chip production. %NOK grows rapidly for LWR values above 5nm.

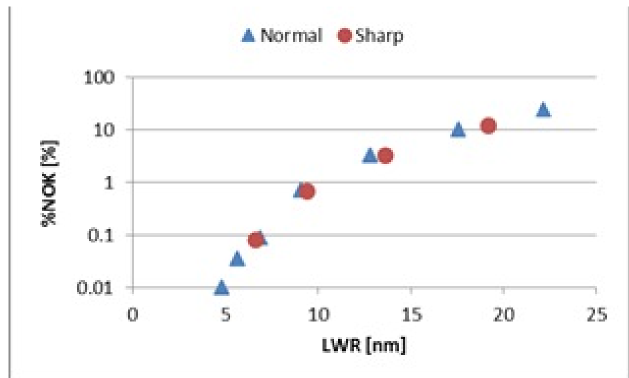

Figure 4. %NOK versus LWR, where triangles represent normal EUV imagery and red circles are for super-sharp step function image. All points with LWR<4.8nm are zero, and not plotted on the log plot.

Downloaded From: http://proceedings.spiedigitallibrary.org/ on 06/07/2017 Terms of Use: http://spiedigitallibrary.org/ss/termsofuse.aspx

An important question is whether LER excursions vary as a normal distribution, as most EPE contributions are assumed to behave. Lithographic specifications are typically checked by measuring hundreds or thousands of data points from which we extract a 3σ value. Then the yield-killing large excursion, e.g. 7σ, is assumed to be very rare based on the rapid fall-off of the normal distribution tails. But what if the true distribution has more extreme excursions than a Gaussian, i.e. "fat tails". In other fields, such as disaster insurance, such events have been called[17] "black swans". They are difficult to study because they are still quite rare events, even though they may be far more likely than predictions based on normal distributions.

With this motivation, let's try to look for evidence of "fat tails" in our LER simulations. Fig. 5 show normal probability plots for three different imaging situations. In such plots, a straight line indicates a normal distribution. Fig. 5a shows the nominal EUV process with LWR=3.76nm. We observe that the distribution is reasonably close to a normal distribution, though there are some small excursions. On the left of the plot, there is a modest departure around 2nm towards smaller CDs, indicative of a slight fat tail. The normal distribution line suggests that we should see minimum CDs on the order of 13nm, but the observed CDs are as small as 11nm. On the right of the plot, there is another slight departure from normality indicating less large CD extremes than the normal distribution line. While the asymmetry is fairly minor, it is in an understandable direction. The fatter tails are seen on the under-exposed small trench CD side, and the skinnier tails are seen on the over-exposed side. Since stochastic noise can be thought of as local exposure dose fluctuations, asymmetry should not be so surprising, since it is well-known that under-exposure is generally more problematic than over-exposure. Fig. 5b is a degraded image using an MSD blur of 4nm which results in an LWR of 4.78nm, right at the cusp where %NOK rises from zero in Fig. 4. Notice that the asymmetry that was slightly present under nominal conditions is now rather strong. On the small CD side, the excursion from a normal distribution is 10 nm, reaching past the 5nm spec limit all the way to CD=0, i.e. definite wire "open" fails. On the large CD side there is again a slight tendency to cut off the largest CDs from the extremes expected for a normal distribution. Finally, in Fig 5c we consider an improved image over the nominal process, where we used the step function image blurred by a 3nm MSD, resulting in an improved LWR value of 2.69nm. This distribution does not have the under-exposed fat tail, and looks to be consistent with a normal distribution over the full range of our data.

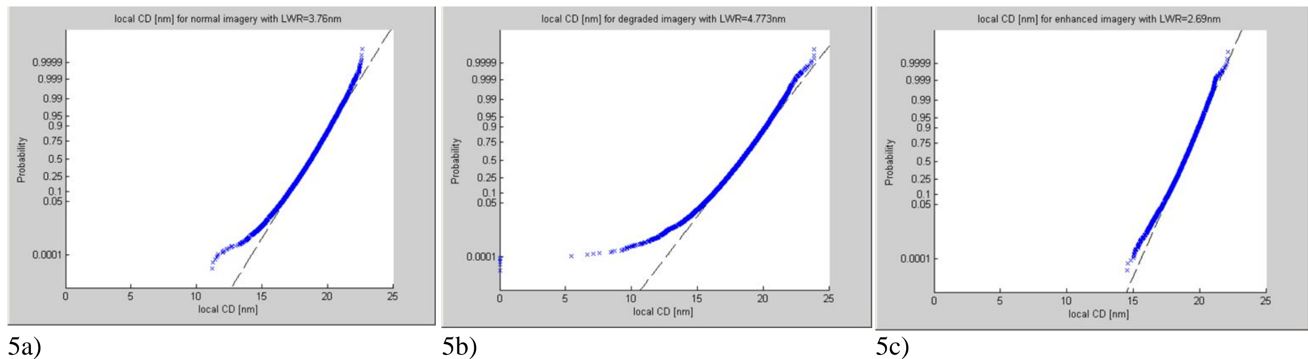

Figure 5. Normal probability plots of local CD distribution for three LWR values: 5a) Normal EUV imagery with LWR=3.76nm; 5b) Degraded EUV imagery with LWR=4.78nm; and 5c) Enhanced EUV imagery with LWR=2.69nm.

Now we look at a different way of degrading the imagery – we simply shrink the mask CD, and do not adjust the dose or any other process parameter. Fig. 6 shows how both the printed mean CD and the ILS value falls with decreasing mask CD. Thus we have two independent factors combining to decrease the yield. The first factor is the smaller CD, bringing the nominal printed linewidth closer to the lower spec limit. For the sake of simplicity, we maintain 5nm as the minimum acceptable local CD throughout this series of simulations. The second factor is that the ILS value is degrading, and so we expect larger LWR and larger stochastic edge fluctuations. Referring back to Fig. 4, notice that when LWR reached 4.8nm (from the MSD blurred images) non-zero %NOK yield loss was detected. Fig. 7 shows the LWR value reaching this critical value when the printed CD shrinks to 17nm or below, and this is where we again detect yield loss in the %NOK value. Thus all of our data – whether from blurred EUV image, whether from blurred step function image or whether from a smaller mask CD – is consistent with LWR controlling yield.

Downloaded From: http://proceedings.spiedigitallibrary.org/ on 06/07/2017 Terms of Use: http://spiedigitallibrary.org/ss/termsofuse.aspx

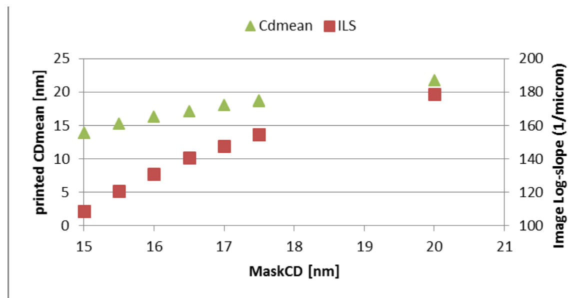

Figure 6. Image log-slope and printed wafer CD at different mask CD. The dose and the process are held constant.

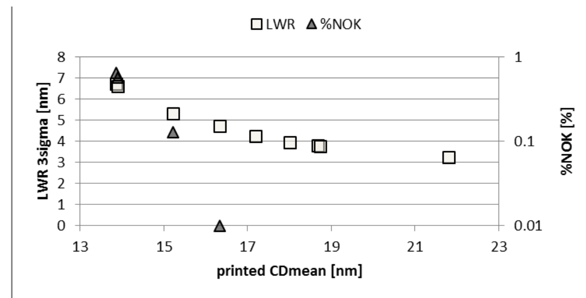

Figure 7. LWR and %NOK plotted versus the printed wafer CD. Zero %NOK values, for CDmean values >16.5nm, are not plotted on this log scale.

Now we examine the CD distributions with the different mask CDs, looking for the on-set of asymmetric non-Gaussian distributions associated with yield loss. The starting point is to review the CD distribution in Fig. 5a, which used the nominal mask CD of 17.5nm. Fig. 8 shows CD distributions for three smaller mask CDs, shrinking from nominal in 0.5nm steps. Fig. 8a, mask CD of 17nm, is qualitatively similar to Fig. 5a, that small CDs occur that are 2nm smaller than expected from the normal distribution line. Fig. 8b, mask CD of 16.5nm shows a larger deviation with the smallest CDs several nm smaller than those expected from normal distribution. Shrinking one more 0.5nm step to maskCD=16nm breaks the process, as Fig. 8c shows up to 10nm smaller CDs than expected from a normal distribution. Any local CD below 5nm is Not OK, and we even see a few occurrences of CD=0. Looking at the whole sequence from mask CD of 17.5nm down to 16nm, we see a slight non-normal distribution step by step become disastrous. The largest CDs in the distribution consistently are smaller than the normal distribution expectation, i.e. a “skinny tail”. The shape of these distributions is quite different from the symmetric, normal distribution that we normally use for yield discussions.

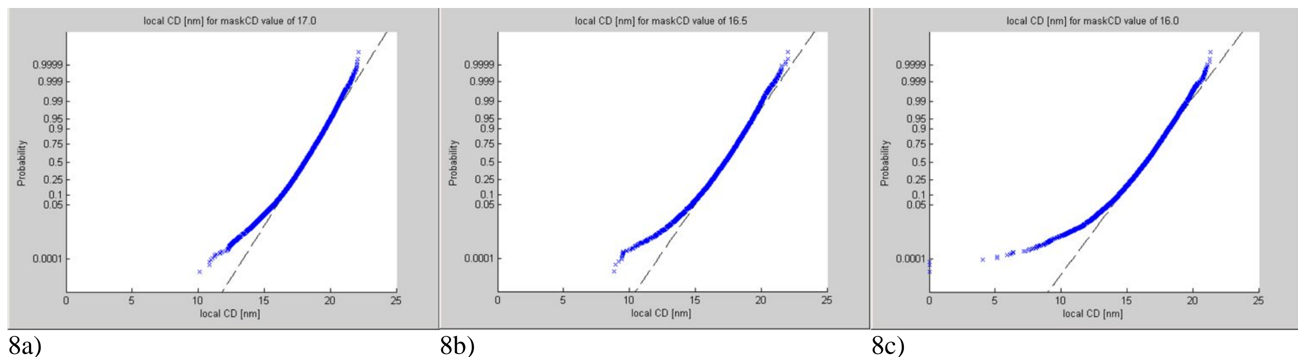

8a) 8b) 8c)

Figure 8. Normal probability plot of local CD distribution for printing with three different mask CD: 8a) EUV imagery with mask CD of 17nm; 8b) EUV imagery with mask CD of 16.5nm; and 8c) EUV imagery with mask CD of 16nm

3. STOCHASTIC EUV RESIST SIMULATIONS OF CONTACT HOLES

Before proceeding with contact hole simulations, we re-analyze the long line simulation results of the previous section in a different way. For calculating LWR we viewed the entire stochastic data set as one 50 micron long line, sliced every 1nm. But we can subdivide the data into segments of any desired length L. For example, we could regard the 50,000 CD slices as 100 lines of length L=500nm, or as 1000 lines of L=50nm length. Now that we have multiple features, we can calculate a Local CD Uniformity (LCDU) which is the 3σ measure of the variation of the mean CD of a large number of features of the same length. We can regard LCDU to be a function of the feature length L, i.e. LCDU(L). We can also calculate an LWR(L) as the Root-Mean-Square of the many LWRs of the individual features of length L. The previous

Downloaded From: http://proceedings.spiedigitallibrary.org/ on 06/07/2017 Terms of Use: http://spiedigitallibrary.org/ss/termsofuse.aspx

section calculated LWR(L=50,000nm) ≈ LWR(L=∞), approximating an infinitely long line. At the opposite extreme, we could view each of the 50,000 slices as individual features, each 1nm long. In this case, LWR(L=1nm) = 0 because there is only 1 local CD value for each feature, and LCDU(L=1nm) = LWR(L=∞), since all of the variation is now viewed as feature to feature.

Fig. 9 plots out LWR(L) and LCDU(L) for a variety of segment lengths L. The LCDU(L) and LWR(L) curve cross at a segment length of L=25nm, which is about 3X the correlation length L_C. So for lines shorter than 25nm, most of the edge roughness will be seen as CD variation from feature to feature. For every L, the LCDU(L) and LWR(L) add up in quadrature to LWR(∞), a kind of conservation of roughness[18, 19].

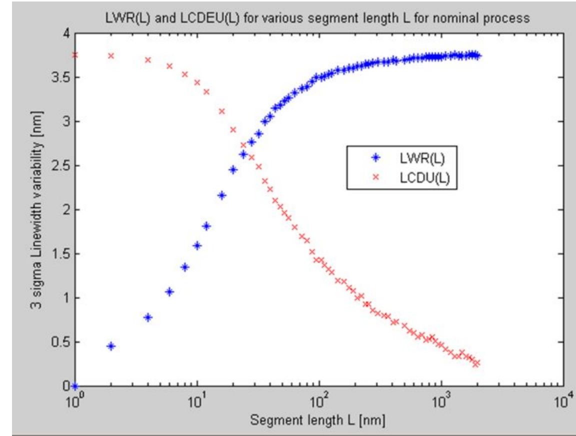

Figure 9. LWR(L) and LCDU(L) plotted versus line length L. 36nm pitch grating printed with nominal process at best dose and focus

A contact hole can be thought of as a very short line, and Fig. 9 suggests that the main impact of roughness on contact holes will be feature-to-feature variation, i.e. LCDU. For our contact hole stochastic study we have chosen a dense hole array on 50nm centers, targeted to print at about 23nm with a mask CD of 24nm at a dose of 72 mJ/cm^2, and using 0.33NA projection optics with a "small annular" source with σ_{outer}=0.643 and σ_{outer}=0.292. 5000 independent simulations of such contact holes were done using the same stochastic resist model used for the long lines of the previous section. Because of stochastic noise, each contact hole has a unique size, shape and center position. Fig. 10 illustrates the distribution of CD and PPE. Fig. 10a shows that the CD distribution is close to a normal one. A small non-Gaussian asymmetry is observed, similar to the long line CDs, where the smallest observed CDs are about 1.5 nm smaller than expected from the normal prediction. On the large CD side, the distribution follows the normal line closely. Fig. 10b shows a scatter plot of the X and Y PPE, showing that the X and Y components are not correlated. Fig. 10c shows a normal probability plot of the PPE-X component indicating that the variation is close to a normal distribution with PPR 3σ=1.79nm, a number which can be compared with a typical 7nm node overall overlay spec of 3σ=3.5nm.

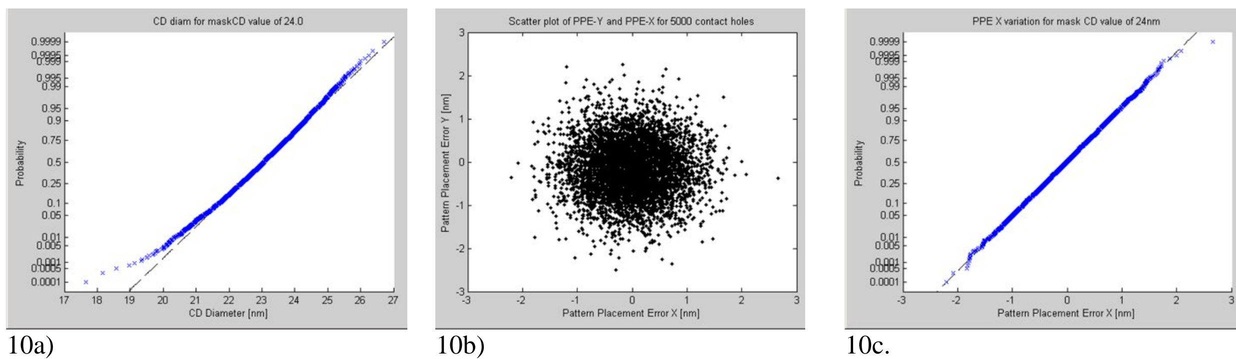

Figure 10. CD and PPE variation for 5000 contact holes with nominal EUV process at best focus and dose: (a) Normal probability plot of CD diameter. The line represents a normal distribution with mean=23.01nm and 3σ=3.12nm; (b) Scatter plot of PPE-Y versus PPE-X for 5000 holes, illustrating stochastic overlay variation; and (c) Normal probability plot of PPE-X. The line represents a normal distribution with mean= -0.01nm and 3σ=1.79nm

Downloaded From: http://proceedings.spiedigitallibrary.org/ on 06/07/2017 Terms of Use: http://spiedigitallibrary.org/ss/termsofuse.aspx

We repeated the hole simulations at seven different values of mask CD, calculating 5000 independent stochastic simulations for each mask CD. Summary results are shown in Table 2. The printed mean CD hole diameter responds strongly as mask CD shrinks, especially at the smallest values which have high Mask Error Enhancement Factor(MEEF). For mask CD values less than 23, the MEEF value exceeds 10! At the nominal mask CD of 24nm, the printed LCDU is 3.12nm, a value similar to the LCDU(L=20nm) value shown in Fig. 9. This suggests that the fundamental edge roughness is quite similar for long line edges and contact hole edges. The LCDU for smaller values of mask CD grows rapidly, especially for the smallest CDs. For determining yield, we again define any CD diameter less than 5nm to be out of specification, i.e. Not OK. Table 2 shows that no detectable fails occur with mask CD of 23.5nm or larger, but below this there is a rapid growth of %NOK. We also track the stochastic overlay fluctuations in both X and Y directions via the PPR 3σ variations in the last two columns of Table 2. The PPR variations steadily grow as the mask CD shrinks.

Fig. 11 describes the CD variation in more detail, with histograms of the 5000 printed hole diameters for each of the seven mask CDs. The overall trends are best seen by scanning the figure from bottom to top. The CD distribution for the largest mask CDs appears to be reasonably symmetric, and there are no missing holes, i.e. CD=0. But as the mask CD gets smaller, the wafer CD distribution becomes broader and more asymmetric, with the left portion of the distribution extending further than the right portion. Most disturbingly, for the two smallest mask CDs, the histogram shows a significant spike at CD=0, *i.e. missing contacts*. This asymmetric distribution of contact hole CDs has been seen in previous stochastic simulations[15]. The overall behavior is quite similar to the behavior of long trench lines seen in the previous section, where the under-exposed side of the distribution has "fatter" tails than the over-exposed side. While for contact holes, the normal probability plots are not shown here, it is obvious that these contact hole CD distributions for small mask CDs are not normal, since they are asymmetric and have discontinuous behavior like the spike at CD=0.

maskCD nm	CD mean nm	LCDU nm	%NOK %	PPR-X nm	PPR-Y nm
22	11.42	19.32	21.7	2.85	2.81
22.5	16.62	11.28	3.7	2.52	2.57
23	19.51	5.13	0.18	2.26	2.25
23.5	21.46	3.51	0	2.02	2.06
24	23.02	3.12	0	1.79	1.89
24.5	24.42	2.82	0	1.69	1.73
25	25.7	2.61	0	1.60	1.61

Table 2. Key metrology results for 5000 independent stochastic holes calculated at each of 7 different mask CD values.

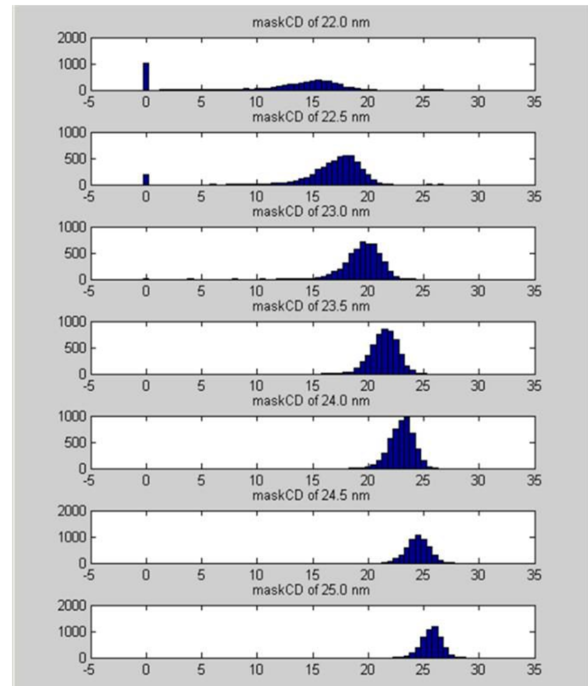

Figure 11. Histograms of CD diameter distribution for seven different values of mask CD, each with 5000 stochastic repetitions.

4. SUMMARY AND FUTURE WORK

EUV lithography simulations were used to illustrate the impact of stochastic fluctuation on CD uniformity, Pattern Placement Error uniformity and yield. The nominal EUV process printed 36nm pitch grating with mean trench CD of 18.73nm, LWR(L=∞)=3.76nm, PPR(L=∞)=1.77nm and no detectable defects according to our simple yield criteria, that the local CD be greater than 5nm and less than 30nm, corresponding to no interconnect opens or shorts. Next we looked at EUV processes with different ILS values. We looked at both normal EUV imagery degraded by various MSD stage blurs, as well as a super-sharp step function image degraded by various MSD, and thus we were able to look at the edge roughness response over a large range of ILS values. We plotted the LWR(L=∞) value versus 0.2/ILS, which gave a smooth universal curve that worked both for the normal EUV imagery as well as the step function image. When we looked at %NOK as a yield metric, we saw that for LWR(∞)<4.8nm there were no detectable errors, i.e. %NOK=0. But

Downloaded From: http://proceedings.spiedigitallibrary.org/ on 06/07/2017 Terms of Use: http://spiedigitallibrary.org/ss/termsofuse.aspx

for LWR> 4.8nm, the %NOK failures rose sharply with increasing LWR. The yield issues were associated with asymmetric non-Gaussian CD distributions, with much "fatter tails" for the smaller CDs (underexposed) compared to the larger CDs (overexposed). Shrinking the mask CD induced similar asymmetric, non-Gaussian distributions and associated yield problems. We also looked at contact hole simulations, and saw that for larger mask CD values, the printed contact hole distribution was reasonably symmetric. But as the mask CD became smaller, asymmetric non-Gaussian distributions were again observed, including CD=0 *missing contact holes*, an obvious yield issue. Both trench long lines and contact holes always failed on the under-exposed side of the CD distribution. For the specific EUV process and features examined in this study, we would recommend the following specs: LWR(∞)<4nm and Image Log-Slope >130/micron.

The simulations presented herein looked for yield issues over relatively small areas: 50,000nm long lines or 5000 contact holes. The critical areas of real chips would be 5 to 6 orders of magnitude larger than this, and do not seem practical for brute force stochastic simulations. Future work is needed to bridge this gap. Extreme value theory or Generalized Pareto Distributions might be useful to fit asymmetric non-Gaussian data, and then extrapolate into large 6σ pattern deviations, i.e. "black swans". Actual yield data of large critical areas will be the ultimate guide, from either ebeam-based pattern inspection metrology or electrical testing. With modern chips needing the order of 10 billion vias, the failure rate per via should be the order of 10^{-12}, i.e. a part per trillion[4]. In such yield studies, it may be useful to degrade the process enough to make failures easier to find. Deliberate "under-exposure" may be the easiest method to controllably degrade the process. Both CD data sets and yield data sets could be obtained for several levels of "under-exposure", and then attempt to correlate pattern failures with asymmetric, non-Gaussian CD distributions, as was done in the present simulation study. The traditional assumption of symmetric Gaussian statistics for CD distributions should be questioned, and verified over as wide a range as possible.

Our work is consistent with the growing realization that LER and stochastic effects will define the limits of lithography[20]. Stochastic phenomena – photon shot noise, resist molecular inhomogeneities, electron scattering events, etc. – now contribute to dimensional variation in EUV resist patterns at levels comparable to or greater than customary sources of variation, such as defocus. These stochastic effects help to limit k_1 to higher values (worse resolution) than traditional optical lithography, and will counteract the benefits of high NA EUV optics. The quest to improve EUV lithography pattern quality will increasingly focus on overcoming stochastic barriers. Higher power EUV light sources[5, 6] are urgently needed as features shrink. Photoresist materials with higher EUV absorption will also help with stochastic issues. Alternative non-polymeric resist materials and post-develop smoothing processes may also play a future role.

ACKNOWLEDGEMENTS

We would like to thank Harry Levinson for suggesting the topic, supporting our team's efforts and providing a broad perspective on the impact of stochastic noise to EUV lithography.

REFERENCES

[1] Obert Wood, "EUV Lithography: Past, Present & Future", International Symposium on EUV Lithography, Hiroshima, Japan(2016).

[2] T. Wallow, C. Higgins et al., "Evaluation of EUV resist materials for use at the 32nm half-pitch node", Proc. SPIE **6921**, paper 6921-1F (2008).

[3] Anna Lio, "EUV Resist Stochastics", EUV Lithography Symposium, IEUVL Resist Meeting, Hiroshima, Japan, (2016).

[4] Gregg M. Gallatin, "Resist blur and line edge roughness", Proc. SPIE **5754**, p. 38 (2005).

[5] Yan Borodovsky, "Life on the edge: EUV insertion challenge", 2012 International Workshop on EUV Lithography, Williamsburg, VA, (2012).

[6] E. Hosler, O. Wood et al., "Considerations for a free-electron laser-based EUV lithography program", SPIE **9422**, 9422-0D (2015).

[7] J. Mulkens, M. Hanna et al., "Overlay and edge placement control strategies for the 7-nm node using EUV and ArF litghoraphy", SPIE **9422**, 9422-1Q (2015).

Downloaded From: http://proceedings.spiedigitallibrary.org/ on 06/07/2017 Terms of Use: http://spiedigitallibrary.org/ss/termsofuse.aspx

[8] Vassilios Constantoudis et al., “Photoresist line-edge roughness analysis using scaling concepts", J. Micro/Nanolith. MEMS MOEMS. **3** (3), 429-435 (2004).
[9] Hiroki Kawada et al., "Key points to measure accurately an ultra-low LER by using CD-SEM ", Proc. SPIE **8681**, 86812N (2013).
[10] Lei Sun, Nicole Saulnier et al. ,"Comparison of left and right side line edge roughness in lithography ", Proc. SPIE **9778**, 9778-22 (2016).
[11] Chris A. Mack, James W. Thackeray, John J. Biafore, and Mark D. Smith, “Stochastic Exposure Kinetics of EUV Photoresists: A Simulation Study”, Journal of Micro/Nanolithography, MEMS, and MOEMS, Vol. **10**, No. 3, p. 033019 (2011).
[12] A. Vaglio Pret, M. Kocsisc, D. De Simone, G. Vandenberghe, J. Stowers, A. Giglia, P. de Schepper, A. Mani, J. J. Biafore, “Characterizing and modeling electrical response to light for metal-based EUV photoresists”, Proc. SPIE **9779**, 9779-5 (2016)
[13] John Biafore, Mark Smith et al., “Statistical simulation of resist at EUV and ArF”, SPIE **7273**, 7273-43 (2009).
[14] P. DeBisschop, J. Van de Kerkhove et al, “Impact of stochastic effects on EUV printability limits”, SPIE **9049**, 9048-09 (2014).
[15] John J. Biafore, Alessandro Vaglio Pret, et al., “Stochastic modeling of EUV resists: simulation of the effects of absorption, quantum yield and photoelectric blur on 18 nm contact hole performance“, IEUVI TWG Resist, Hiroshima, (2016).
[16] Figure 2 of reference 8.
[17] Nassim Taleb, [The Black Swan: Second Edition: The Impact of the Highly Improbable], Random House (2010).
[18] Yuansheng Ma ; Harry J. Levinson and Thomas Wallow, "Line edge roughness impact on critical dimension variation", Proc. SPIE **6518**, Metrology, Inspection, and Process Control for Microlithography XXI, 651824 (2007).
[19] Chris A. Mack, “Analytical Expression for Impact of Linewidth Roughness on Critical Dimension Uniformity”, Journal of Micro/Nanolithography, MEMS, and MOEMS, Vol. 13, No. 2, p. 020501 (2014).
[20] Chris A. Mack, “Line-Edge Roughness and the Ultimate Limits of Lithography”, SPIE **7639** p. 763931 (2010).

Downloaded From: http://proceedings.spiedigitallibrary.org/ on 06/07/2017 Terms of Use: http://spiedigitallibrary.org/ss/termsofuse.aspx